applied sciences

MDPI

Article

Patient-Specific Dosimetry Evaluations in Theranostics Software for Internal Radiotherapy

Elisa Grassi [1], Domenico Finocchiaro [2], Federica Fioroni [1,*], George Andl [3], Angelina Filice [4], Annibale Versari [4], Ayman El Ouati [5], Emiliano Spezi [6] and Mauro Iori [1]

[1] Medical Physics Unit, Azienda USL-IRCCS di Reggio Emilia, 42123 Reggio Emilia, Italy; elisa.grassi@ausl.re.it (E.G.); mauro.iori@ausl.re.it (M.I.)
[2] Medical Physics Unit, University Hospital of Modena, 41124 Modena, Italy; finocchiaro.domenico@aou.mo.it
[3] Varian Medical Systems Inc., 3100 Hansen Way, Palo Alto, CA 94304, USA; george.andl@varian.com
[4] Nuclear Medicine Unit, Azienda USL-IRCCS di Reggio Emilia, 42123 Reggio Emilia, Italy; angelina.filice@ausl.re.it (A.F.); annibale.versari@ausl.re.it (A.V.)
[5] Department of Physics, University of Modena and Reggio Emilia, 41125 Modena, Italy; ayman.elouati@gmail.com
[6] School of Engineering, Cardiff University, Cardiff CF24 3AA, UK; espezi@cardiff.ac.uk
* Correspondence: federica.fioroni@ausl.re.it; Tel.: +39-0522-296653

Abstract: In Internal Radiotherapy, radiopharmaceutical dosimetry provides an accurate estimation of absorbed radiation doses to organs at risk and tumours. In this paper Velocity Theranostics (Varian Medical Systems), is investigated. Its performances are compared to OLINDA 2.0 in both an anthropomorphic phantom and a group of patients. Velocity Theranostics was evaluated with a cohort of patients (15) treated with ^{177}Lu radiolabelled peptides. The absorbed doses were calculated for the liver, spleen and kidneys, separately with OLINDA 2.0 and Velocity Theranostics using the same set of images. To reduce the contribution of Time-integrated activities (TIAs) on the results and to merely compare the dose calculation algorithms, the OLINDA 2.0 absorbed doses were calculated using the TIA values calculated in Velocity Theranostics. The absorbed doses from Velocity Theranostics were found to be correlated with the doses from OLINDA 2.0 with the TIAs from Theranostics (Lin's coefficient = 0.894 and R^2 = 0.9531). Absorbed doses from Velocity Theranostics are reliable at least as reliable as those for OLINDA 2.0, with many advantages regarding accuracy of calculations and robustness. In conclusion, the personalisation of dosimetry may be totally fulfilled by computational systems for absorbed dose in internal radiotherapy, equipped with a complete workflow and borrowed from external radiotherapy.

Keywords: internal radiotherapy; dosimetry; ^{177}Lu; theranostics; software

Citation: Grassi, E.; Finocchiaro, D.; Fioroni, F.; Andl, G.; Filice, A.; Versari, A.; El Ouati, A.; Spezi, E.; Iori, M. Patient-Specific Dosimetry Evaluations in Theranostics Software for Internal Radiotherapy. *Appl. Sci.* **2024**, *14*, 7345. https://doi.org/10.3390/app14167345

Academic Editor: Lorenzo Manti

Received: 2 July 2024
Revised: 24 July 2024
Accepted: 27 July 2024
Published: 20 August 2024

1. Introduction

Internal radiotherapy (IR) currently represents a growing field of nuclear medicine [1], which has rapidly evolved over the last few years. Radiolabelled vectors administered in IR concentrate cytotoxic quantities of radioactivity selectively in targets, preserving simultaneously the adjacent healthy tissues.

At the same time radiopharmaceutical dosimetry has been evolving [2], providing an increasingly accurate estimation of absorbed radiation doses to healthy organs and tumours. The work of Peters S. et al. [3] shows an overview of the practice of dosimetry for IR in Europe, concluding that there is a large variation in the practice of IR across and within countries. However, the general increase in the application of IR and the implementation of the Council Directive 2013/59/Euratom and other position papers is likely leading to modifications in the practice of dosimetry in the next few years, to ensure the standardisation of dosimetry for IR [4,5].

Temporal and spatial biodistributions of administered radiopharmaceuticals are assessed as accurately as possible from clinical quantitative imaging used in radiopharmaceutical dosimetry. Throughout the calculations a few challenges are met at some stage in the process (i.e., accurate image quantification, image registration, or time activity integral calculations) and specific uncertainties can be associated with the resulting absorbed doses [6,7]. The robustness of each step of dosimetry achieves more accurate absorbed dose estimations.

Existing software tools for dosimetry calculations differ significantly in design, functionality and degree of personalization and are typically grounded on a variety of models and assumptions, ranging from simple look up table (as in the case of ICRP 128) to computationally heavy Monte-Carlo codes for radiation transport calculations [8,9].

Dosimetry can be performed at different scales, ranging from volumetric level (whole-body or organ based), to voxel size and lower to cellular size.

Dosimetry software for calculation at organ level has been used for many years as a unique solution for dosimetry: OLINDA/EXM [10] version 1.0 code for personal computer was the first piece of software implementing a standardised dosimetry schema in internal dosimetry.

More recently, several software packages have become available for dosimetric applications in IR, such as IDAC-Dose 2.1 [11] and MIRD-calc [2]. Aside from that, kernel convolution and Monte Carlo-based tools have been implemented in the last few years [12,13].

In favour of the implementation of voxel level techniques, some studies indicate that deterministic biologic effects are mispredicted by the mean absorbed dose alone and may be significantly conditioned by not homogeneous dose distributions [14].

Currently most IR treatments consist of the administration of a fixed activity, such as in the case of [^{177}Lu]Lu-DOTATATE (Lutathera, Novartis) for the treatment of neuroendocrine tumours (4×7.4 GBq injections separated by 8 weeks intervals). Though the administration of fixed activities is not compliant with the rules of a personalised treatment, in which the optimal activity is chosen individually for each patient, the verification of the delivered absorbed dose can be assessed after administration [12]. Even if performed as verification, dosimetry improves the knowledge of the relationship between absorbed dose and clinical effect, as a prediction of the therapy outcome [15].

Since dosimetry hold an important position in personalised medicine, the use of an advanced software is relevant, because it allows covering all of the necessary steps in one environment (i.e., image registration, volume of interest contouring, absorbed dose computation and therapy planning) and because it most likely represents a robust technique to carry out accurate dosimetry.

In this paper Velocity Theranostics, a piece of commercial software, developed by Varian Medical System (Varian Medical Systems, Palo Alto, CA, USA) as advanced dosimetry software, is presented. It can perform structure-based calculations (according to MIRD/RADAR schema, which is also adopted by OLINDA), and voxel-based dosimetry calculations. Velocity Theranostics adopts a novel absorbed dose calculation algorithm based on Linear Boltzmann transport equation. This approach can be considered as a gold standard method, since it incorporates high accuracy calculations equivalent to MC methods, but with faster computational speed (similar to the speed of kernel convolution methods).

In this study, Velocity Theranostics performances were compared with OLINDA 2.0 [16]. Dose calculations were performed using images of phantoms and patients.

2. Materials and Methods

OLINDA 2.0

OLINDA/EXM version 2.0 software (OLINDA 2.0) implements the RADAR method for internal dose assessment [16]. It is used to estimate mean absorbed doses to organs or lesions, through the use of tabulated S-values and computational phantoms (e.g., adult male and adult female for organs' estimates) or specific models (e.g., sphere model for lesions' estimates), with a low level of personalization.

OLINDA 2.0 uses a series of voxel-based, realistic human computational phantoms developed by RADAR committee of SNMMI (Society of Nuclear Medicine and Molecular Imaging), which are based on 2007 ICRP (International Commission on Radiological Protection) recommendations. Compared to the previous versions of OLINDA/EXM, OLINDA 2.0 implements the most recent biokinetic models. The concepts on which OLINDA 2.0 works are identical to the MIRD method for internal dosimetry. However, MIRD and RADAR methods use different terminologies [16].

Velocity Theranostics

Velocity Theranostics is a piece of research software available on the Velocity 4.0 workstation produced by Varian Medical Systems (Palo Alto, USA) capable of estimating and reporting doses in selected structures at organ-level (in terms of mean absorbed dose) or at voxel-level (e.g., dose distributions in organs). The Linear Boltzman equation solver performs a voxel based calculation, and the mean absorbed dose is also reported.

Velocity Theranostics provides all the necessary steps to perform internal dosimetry, from clinical images to absorbed dose calculations.

The workflow of the Theranostics calculations includes the following steps, which are also shown in Figure 1:

1. **Volume delineation:** Volume of interest (VOI) delineation of Organ at Risk (OAR) and/or lesions is performed using the Velocity contouring tool. This tool enables the user to choose among different options, such as manual contouring, adaptive semi-automatic and threshold-based.
2. **Image registration:** Sequential SPECT/CT images are automatically registered with a deformable algorithm based on CT data.
3. **Activity quantification:** The counts–to-activity calibration factor (CF) is entered by the user. It can be extrapolated by acquiring a homogeneous phantom filled with a radioactive solution with the SPECT clinical protocol.
4. **CT Calibration**: The accuracy of the calibration of CT numbers in relation to electron density is a relevant factor for absorbed dose calculations in a not homogeneous medium. It is possible to verify and customize the conversion of Hounsfield units (HU) into material composition and mass density using a tissue characterization phantom.
5. **Partial Volume Effect (PVE) correction**: This can be applied by entering an equation which allows to estimate the recovery coefficients for VOI statistics, that are specific for the SPECT scanner in use.
6. **Time-integrated activities (TIAs):** The algorithm uses a fitting technique at voxel level, which estimates a fitting function (sums of exponentials) for each voxel, This process automatically selects the best model from a predefined list of possibilities, using the Akaike Information Criterion (AIC) [17]. The algorithm provides an error metrics statistics section based on the calculation of the symmetric mean absolute percentage error (SMAPE), which allows measuring the accuracy in terms of percentage (or relative) errors.
7. **Absorbed dose calculated with Acuros MRT algorithm:** This deterministic solver is customized for internal therapies. It includes the solution of the linear Boltzmann transport equation (LBTE) for photons and the linear Boltzmann-Fokker-Planck transport equation (LBFPTE) for electrons and it takes into account that photon and electron energies for internal therapy applications are significantly lower than the energies used in external beam radiation therapy applications. The performances of the LBTE solver for internal therapies with ^{177}Lu were considered and described in-depth by Kayal G. et al. [18]. The algorithm may perform voxel dosimetry. The resulting dose maps and dose-volume-histograms are then internally elaborated to provide the mean doses absorbed by the structures delineated on SPECT-CT images (organs and lesions). These values may be compared to the absorbed doses calculated by OLINDA 2.0.

Step 1: Volume delineation and image registration

Step 2: Activity quantification

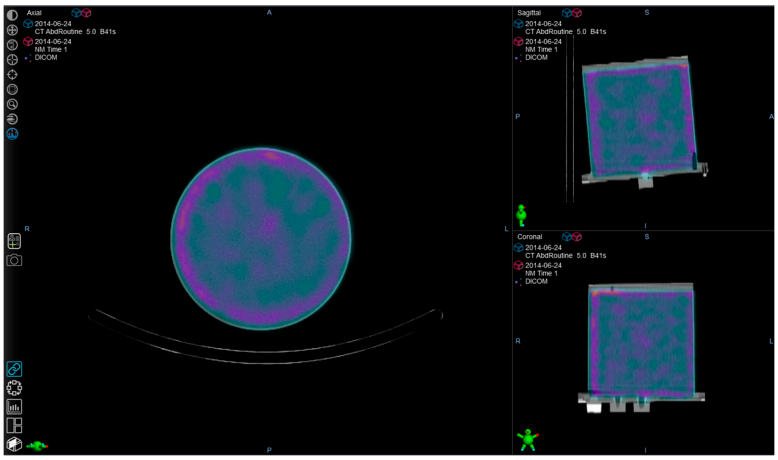

Step 3: TIAs

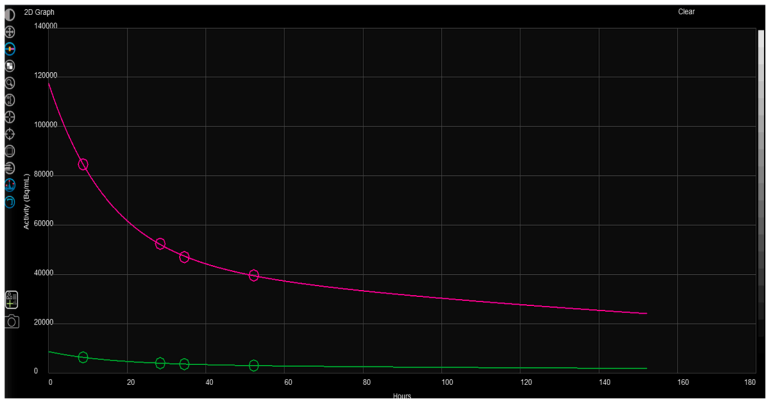

Figure 1. *Cont.*

Step 4: Absorbed dose calculation

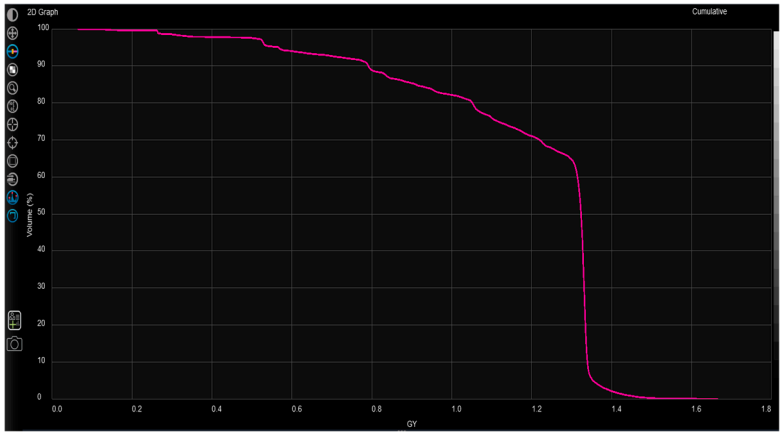

Figure 1. Workflow of the Velocity Theranostics calculations.

Phantom

The manlike phantom Liqui-Phill (The Phantom Laboratory, Greenwich, NY, USA) provided with 4 inserts (Left kidney, Right kidney, Liver and Spleen) was chosen to evaluate Velocity Theranostics. For this purpose in each insert a specific ^{177}Lu activity concentration was injected, as shown in Table 1. This antropomorphic phantom was acquired once with a SPECT/CT tomograph (Figure 2), while later on a set of 4 SPECT/CT images was generated (using Matlab, The MathWorks Inc., Natick, MI, USA) for the purpose of simulating radiopharmaceutical bio-kinetics. The time points were generated to simulate scans at 1 h, 4 h, 24 h, 48 h and 70 h post injection.

During the preparation of the phantom, to ensure the accurate measure of the volumes, a calibrated scale was used to measure the weight of phantom and inserts (before and after refilling). The density of the solution of water and radioactivity was considered as 1 g/mL. HCl (0.1 M) was injected to water as a carrier solution so as to avoid ^{177}Lu deposition on the phantom walls and to ensure a more uniform radioactive solution.

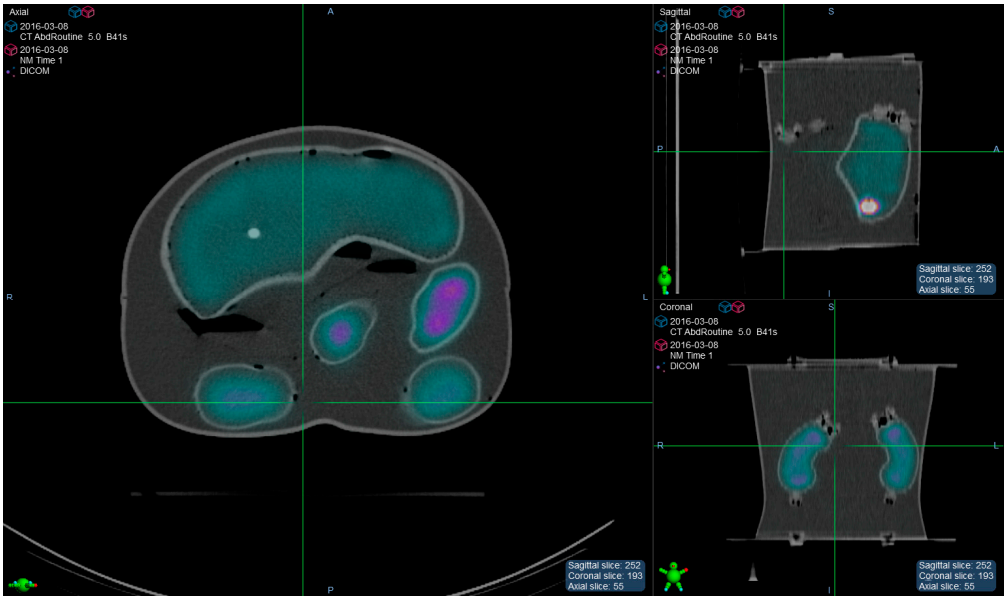

Figure 2. SPECT-CT scan of Liqui-Phill phantom.

Table 1. Activities used to fill Liqui-Phill phantom.

Phantom	Phantom Volume (mL)	Insert Name	Insert Volume (mL)	Insert Activity Concentration (MBq/mL)	Background Activity Concentration (MBq/mL)
Liqui-Phill phantom	11,600	Left kidney	142	0.81	0.03
		Right kidney	142	0.82	
		Spleen	156	1.10	
		Liver	1470	0.53	

Cohort of Patients

Velocity Theranostics was evaluated with a cohort of clinical cases (15), who were extracted from the group of patients enrolled in a clinical PRRT trial (EUDRACT 2015-005546-63) at AUSL-IRCCS of Reggio Emilia (Italy), who gave written informed consent for dosimetry calculations.

Dosimetry was scheduled on the occasion of the first course of therapy following a therapeutic administration of ^{177}Lu-labelled peptides. Each patient underwent 4 SPECT/CT scans at approximately 1, 24, 40 and 75 h post injection for dosimetry purpose. Absorbed doses were calculated for liver, spleen and kidneys.

Image Acquisition and Reconstruction

A SPECT-CT scanner (Symbia T2, Siemens Healthineers Headquarters, Forchheim, Germany, 3/8" NaI(Tl)-detector) which was previously calibrated for ^{177}Lu (CF = 28.5 Bq/count) [19] was used to perform image acquisitions of phantom and patients through a clinical protocol for body studies. It uses: MEHR collimators; 128 × 128 matrix; zoom = 1; views = 32 × 2; time/view = 30 s; step and shoot mode; degree of rotation = 180°; non-circular orbit; detector configuration = 180°. The first clinical CT image was acquired with 130 kV and 90 mAs, using tube current modulation. The following CT images were acquired at 130 kV with a fixed value of 40 mAs to respect the safety of the patient. The slice thickness of reconstructed images was 5 mm. A smooth reconstruction kernel was used (B08s; Siemens Medical Solution, Germany).

The iterative algorithm Flash 3D (10 it.; 8 sub.; Gaussian filter 4.8 mm; cubic voxel size 4.8 mm) [20] was used to reconstruct SPECT images in Siemens E-Soft workstation (Syngo, MI Application version 32B, Siemens Healthineers Headquarters, Forchheim, Germany) with CT based attenuation correction, scatter correction and collimator-detector response correction.

Data Analysis and Statistics

The absorbed doses were computed independently with OLINDA 2.0 and Velocity Theranostics (organ-level option) using the same set of images for both for the anthropomorphic Liqui-Phill phantom and for clinical cases. The Time-Integrated Activity used for OLINDA 2.0 absorbed dose calculations were computed in Matlab using a bi-exponential curve to fit the time-activities data extrapolated from Velocity segmentation tool.

In addition and only in the study of the cohort of patients, OLINDA 2.0 absorbed doses were calculated again using the TIA values calculated in Velocity Theranostics, with the purpose of reducing the contribution of the TIA on the results and to merely compare the dose calculation algorithms. In the following, these absorbed doses are named as OLINDA$^{(\text{Theranostics TIA})}$. Flowchart in Figure 3 schematically shows the methodology of the absorbed dose calculation in the clinical study.

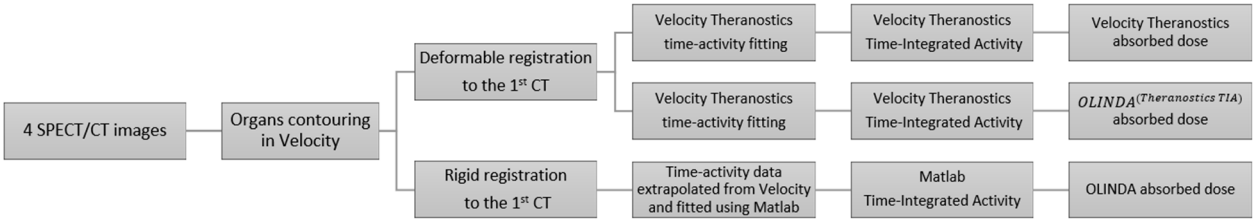

Figure 3. Schema of the methodology adopted in the absorbed dose calculation in the cohort of patients.

Correlations between the calculations performed with OLINDA 2.0 and Thernostics were evaluated by means of the Lin's concordance coefficient (LC), while the agreement between the methods was studied using the Bland-Altman plot. Perfect concordance corresponds to a value of LC equal to +1, perfect discordance corresponds to a value equal to −1, while no correlation corresponds to a value of 0. For statistical analysis MATLAB R2023B (The MathWorks Inc., Natick, MI, USA) was used.

3. Results

Phantom Study

Mean absorbed doses and TIAs of the phantom calculated with OLINDA 2.0 and Velocity Theranostics are included in Table 2 and plotted in Figure 4.

Table 2. TIAs and Absorbed doses for the phantom.

Insert Name	TIA (MBq h/MBq)			Absorbed Dose (Gy)		
	Olinda 2.0	Velocity Theranostics	Difference (%)	Olinda 2.0	Velocity Theranostics	Difference (%)
Kidneys	34.8	34.5	−0.9	17.5	16.9	−3.5%
Spleen	32.6	32.1	−1.56	31.44	30.06	−4.4%
Liver	136	149.8	10.2	13.68	14.46	5.7%

Figure 4 shows the results concerning the inserts positioned in the Liqui-Phill phantom.

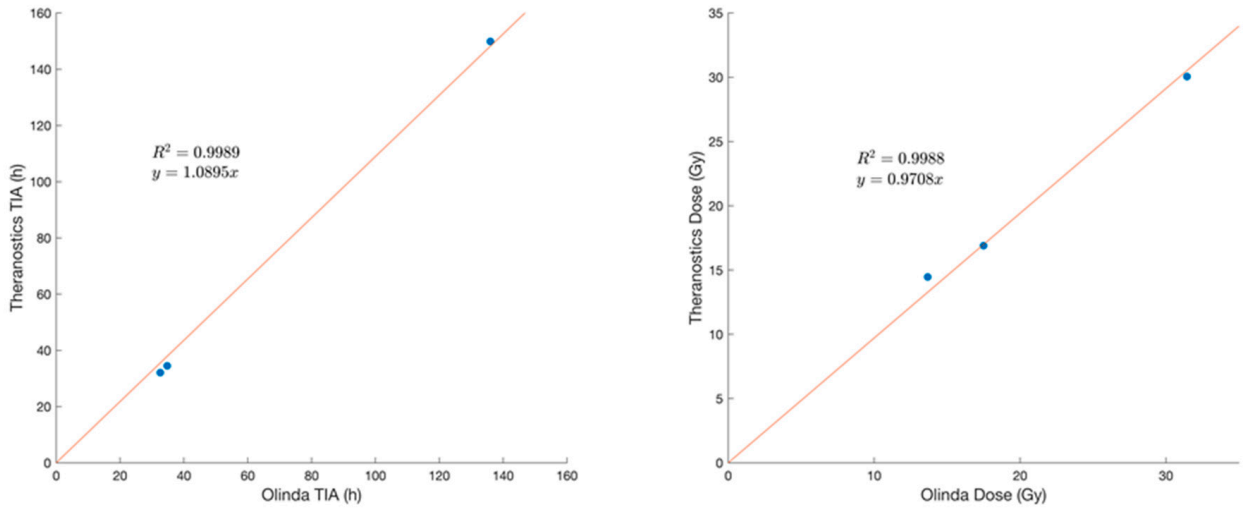

Figure 4. Dispersion graph of the results (for TIA and dose calculations) regarding the inserts placed in the Liqui-Phill phantom.

Clinical Cases

The absorbed doses in OLINDA 2.0 and Velocity Theranostics for the kidneys, spleen and liver of the cohort of patients are shown in Table 3. TIAs and absorbed doses calculated with OLINDA 2.0 and Velocity Theranostics are plotted in Figure 5.

Table 3. Mean absorbed doses (Gy/GBq) calculated with OLINDA 2.0, Velocity Theranostics, OLINDA 2.0 with TIAs of Velocity Theranostics (OLINDA$^{(\text{Theranostics TIA})}$) for kidneys, liver and spleen.

Case	Kidneys			Liver			Spleen		
	Olinda 2.0	Velocity Theranostics	OLINDA$^{(\text{Theranostics TIA})}$	Olinda 2.0	Velocity Theranostics	OLINDA$^{(\text{Theranostics TIA})}$	Olinda 2.0	Velocity Theranostics	OLINDA$^{(\text{Theranostics TIA})}$
1	0.304	0.467	0.461	0.0605	0.705	0.643	—	—	—
2	0.440	0.373	0.464	0.295	0.259	0.316	—	—	—
3	0.575	0.464	0.529	0.136	0.187	0.195	0.563	0.341	0.459
4	0.321	0.341	0.448	0.398	0.341	0.396	0.619	0.574	0.851
5	0.253	0.551	0.719	0.110	0.176	0.203	0.145	0.383	0.427
6	0.519	0.483	0.567	0.0806	0.155	0.175	0.730	0.579	0.758
7	0.250	0.420	0.482	1.700	1.110	1.44	0.63	0.408	0.642
8	0.593	0.453	0.731	0.110	0.165	0.164	—	—	—
9	0.540	0.646	0.761	0.902	1.110	1.29	0.563	0.508	0.657
10	0.385	0.320	0.406	0.341	0.235	0.287	1.050	0.558	0.837
11	0.529	0.499	0.537	1.740	1.090	1.240	1.780	0.651	0.903
12	0.544	0.774	0.852	0.0793	0.112	0.112	0.410	0.330	0.302
13	0.620	0.646	0.752	0.0661	0.0793	0.0843	0.434	0.411	0.477
14	0.662	0.684	0.760	0.163	0.177	0.184	0.631	0.550	0.644
15	0.341	0.319	0.389	0.130	0.141	0.158	0.441	0.425	0.566

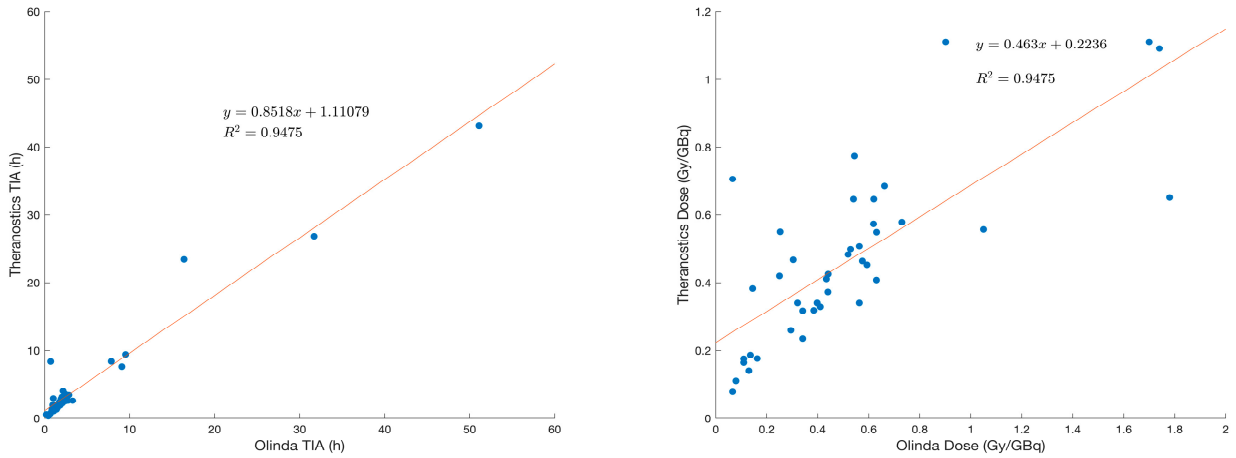

Figure 5. Dispersion graph of the results for the complete cohort of patients for TIA and absorbed dose.

Figures 6 and 7 show the results of the second comparison between absorbed doses. The data included in the columns denoted as "OLINDA 2.0 with TIAs of Velocity Theranostics" (OLINDA$^{(\text{Theranostics TIA})}$) in Table 3 were considered in place of data in the columns denoted as "OLINDA 2.0". For this purpose, OLINDA 2.0 was run while inserting the same TIA values calculated by Velocity Theranostics, to better investigate the performance of the dosimetry algorithm of Velocity Theranostics.

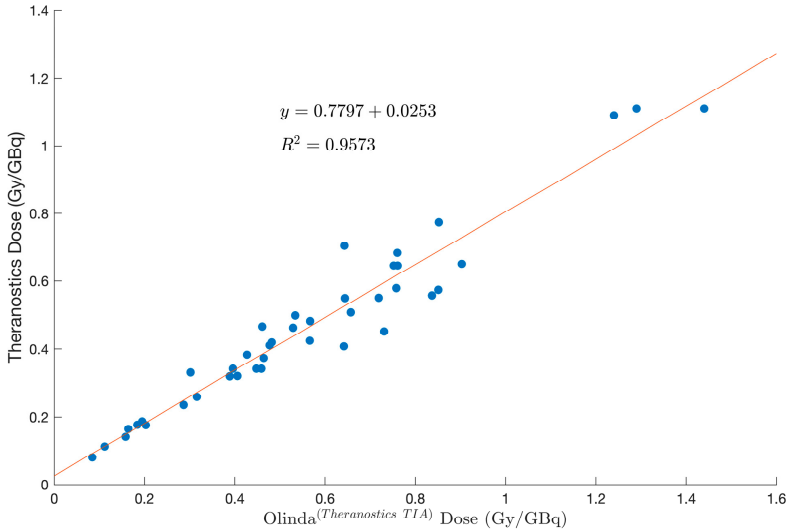

Figure 6. Dispersion graph of the results for the cohort of patients for absorbed doses calculated by running OLINDA 2.0 with the same TIA values calculated by Velocity Theranostics.

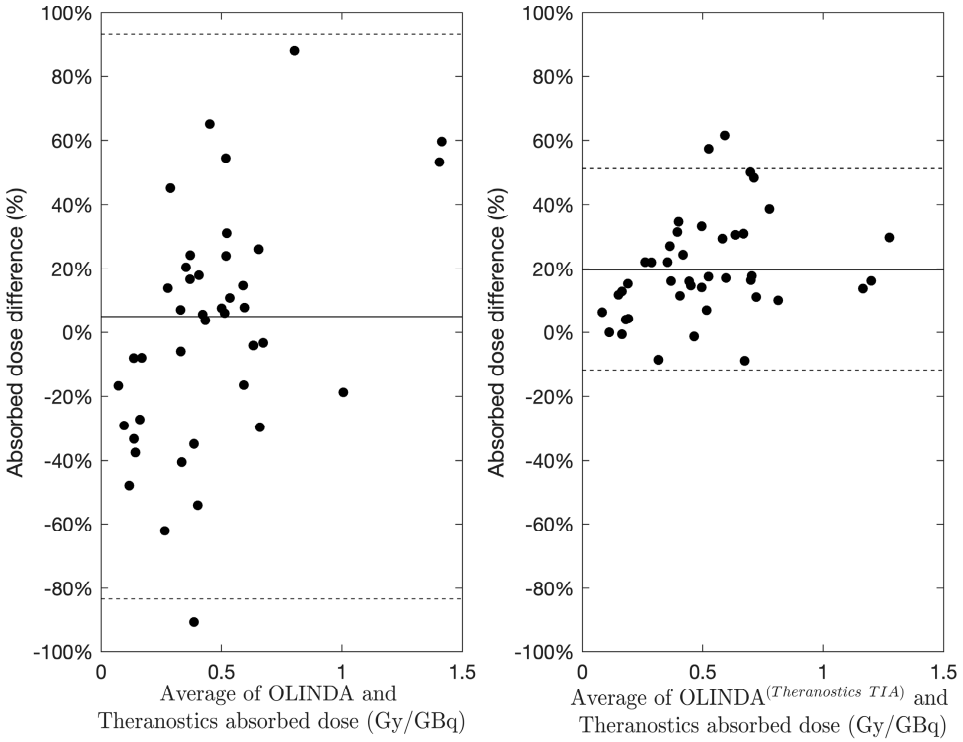

Figure 7. Bland-Altman plots for absorbed doses of Theranostics vs OLINDA 2.0 (on the left) and OLINDA$^{(\text{Theranostics TIA})}$ (on the right). The difference was evaluated as the percentage difference of Velocity Theranostics in comparison with the OLINDA 2.0 dose. Dashed lines represent the limits of agreement (±1.96 SD). The horizontal solid lines represent the average percentage differences.

The Bland–Altman analysis in Figure 7 shows lower differences when the same TIA is used in absorbed dose calculations (OLINDA$^{(\text{Theranostics TIA})}$). This is also evident in Figure 8, where differences (%) are visually compared using box-plots.

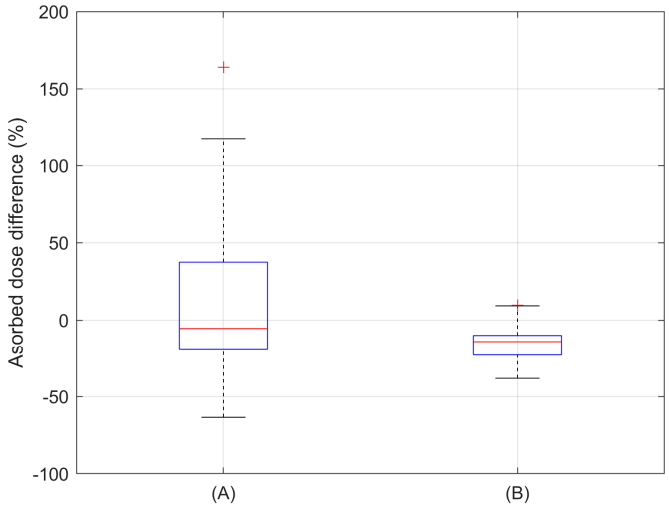

Figure 8. Box-plots representing the absorbed dose percentage difference calculated in the cohort of 15 patients between Velocity Theranostics and both OLINDA 2.0 (A) or OLINDA$^{(\text{Theranostics TIA})}$ in (B).

The absorbed doses were found to be poorly correlated (Lin's coefficient = 0.672) between OLINDA 2.0 and Velocity Theranostics, while better correlation was found between OLINDA$^{(\text{Theranostics TIA})}$ and Velocity Theranostics (Lin's coefficient = 0.894).

4. Discussion

In this study we compared Velocity Theranostics to OLINDA 2.0, with the aim to evaluate the advantages of using advanced software for absorbed dose assessment in IR.

This comparison was performed in ideal conditions (i.e., acquisition/processing of a radioactive phantom) and in more realistic conditions, through a selection of patients chosen from a clinical trial.

Clinical conditions are quite distant from the ideal conditions achievable in a phantom, namely in terms of biological kinetics, multiple sequential acquisitions of SPECT/CT images, image registration issues [21], image artefacts caused by patient motion, irregular volumes of interest, not homogeneous activity distribution. To be as close as possible to clinical situations, a synthetic dataset of images was created, generating kinetics for organs similar to clinical kinetics, starting from the image of an anthropomorphic phantom. This choice was driven by the need to have a time activity curve for organs similar to clinical cases (supposing a bi-exponential decay), as reference for the calculations of TIAs and absorbed doses. Furthermore, homogeneity of activity distribution inside inserts permits making the comparison between two different calculation approaches more robust.

As reported in Table 2, the percentage differences in the phantom ranged from −0.9% to 10.2% for the TIAs and from −4.4% to 5.7% for absorbed doses.

The data are plotted in Figure 4, showing a high correlation both for TIAs and doses (R^2 = 0.9968 and 0.9902, respectively).

These results highlight the good agreement between the two calculation techniques, with no specific overestimation or underestimation.

In relation to the analysis of clinical cases, data concerning the comparison between Velocity Theranostics and OLINDA 2.0 are plotted in Figure 5, showing a high correlation for the TIAs (R^2 = 0.9475) and a lower correlation for the doses (R^2 = 0.5856).

Data related to the comparison between Velocity Theranostics and OLINDA 2.0 run with the same TIA values calculated by Velocity Theranostics (OLINDA$^{(\text{Theranostics TIA})}$) are reported in Figure 6. It shows a high correlation for the doses (R^2 = 0.9531) which is decisively stronger than the correlation shown in Figure 5 for the comparison with OLINDA 2.0, as described in Materials and Methods.

Even the Bland-Altman plots for both comparisons (Figure 7) show the reduction in the percentage absorbed dose differences in the case of using the same TIAs as Velocity Theranostics.

Similarly Figure 8 highlights the reduction of the absorbed dose percentage differences for the cohort of patients.

Lin's coefficient of concordance confirmed better agreement with the calculations in the case of same TIAs of Velocity Theranostics being used.

The main reasons for the dispersion of data for absorbed doses shown in Figure 5 can be attributed to different steps of dosimetry computation [6], which add uncertainties to the absorbed dose estimations.

The registration of the images used for the dosimetry with OLINDA 2.0 was rigid, while Velocity Theranostics used deformable registration. As reported in [22], deformable algorithms provide a better registration than the rigid algorithm, generating an image more similar to the reference one. Aside from that, it was concluded that deformable registered images generate a structural similarity index measure (SSIM) more stable than the rigidly reconstructed images. The rigid registrations may be indeed difficult because of patient repositioning for sequential acquisitions or because of patient movements during acquisitions. Furthermore, rigid registration can be defined "locally" accurate, while deformable registration can be defined "globally" accurate, since it takes into account multiple internal organ movements.

Concerning curve fitting, it was stated in Finocchiaro's paper [6] that this is one of the most relevant sources of uncertainties. Many options exist for curve fitting [23], including modelling software, such as SAAMII (version 2.0 or higher), or Olinda/EXM (version 1.0 and higher), or advanced software, such as MATLAB (version 2020 or more recent), or Python (version 3.12.4 is now available).

Preparation of biokinetic data and choice of the appropriate error model are the starting point of fitting calcuations. In this context, Velocity Theranostics provide complete error metric statistics, calculating the Symmetric Mean Absolute Percentage Error (SMAPE). This is an important tool for estimating the goodness of the curve fitting.

In this work a unique set of structures for organs was used in both techniques, so that VOIs could not represent a source of uncertainties, limited to this study.

Velocity Theranostics has the advantage of using the Acuros MRT algorithm, based on the interactions of radioactive particles with matter, which considers a source and a radiation transport model applied to IR. Aside from that, Acuros MRT takes into account density and type of material, through the Hounsfield Unit (HU) of the CT images. In clinical cases, patient anatomy provides specific information on materials, which permit to calculate the radiation transport in the matter (e.g., CT tissue segmentation based on density ranges).

Fogliata et al. [24] demonstrated a good agreement between Acuros MRT and Monte Carlo approaches and concluded that Acuros MRT is an effective alternative to Monte Carlo.

In this paper we presented the comparison with OLINDA 2.0, which is the reference for dosimetry computation in IR. However, OLINDA 2.0 cannot provide a complete personalised dosimetry, since it uses standard anthropomorphic phantoms and considers only homogeneous distributions of activity. The differences obtained in this paper between Velocity Theranostics and OLINDA 2.0 with TIAs from Velocity Theranostics ($OLINDA^{(Theranostics\ TIA)}$) may mainly be due to these aspects.

Theranostics software, such as other commercially available software, meets the need of a complete workflow for dosimetry from image elaborations to absorbed dose distributions. For this reason, these kinds of software turn out to be more robust and reliable than the use of multiple tools to calculate TIAs for OLINDA 2.0.

5. Conclusions

This study showed results for organ-level dosimetry calculated with different modalities, namely when using advanced software (Velocity Theranostics) and OLINDA 2.0.

The differences between the two modalities decreased significantly when OLINDA 2.0 was run with the same TIAs calculated by Velocity Theranostics (OLINDA$^{(\text{Theranostics TIA})}$), therefore highlighting the true discrepancies of the computation techniques.

In conclusion, the personalisation of dosimetry may be totally fulfilled by computational systems for absorbed doses in IR, equipped with a complete workflow and borrowed from external radiotherapy.

Author Contributions: E.G., D.F., F.F., A.E.O., M.I., E.S. and G.A. contributed to the design of the study; E.G., D.F. and F.F. contributed to the manuscript preparation; A.F. and A.V. contributed to image analysis and preparation; E.G., D.F., F.F. and A.E.O. contributed to data analysis; G.A. contributed to the manuscript review. All authors have read and agreed to the published version of the manuscript.

Funding: This research received no external funding.

Institutional Review Board Statement: This study was conducted according to the guidelines of the Declaration of Helsinki and approved by the Ethics Committee of AUSL-IRCCS of Reggio Emilia (Italy) (EUDRACT 2015-005546-63).

Informed Consent Statement: Informed consent was obtained from all subjects involved in the study.

Data Availability Statement: The data presented in this study are available on request from the corresponding author.

Acknowledgments: This study was partially supported by the Italian Ministry of Health's Ricerca Corrente Annual Program 2025.

Conflicts of Interest: George Andl is an employee of Varian Medical Systems, a Siemens Healthineers company. No other authors have any potential conflict of interest relevant to this article.

References

1. Sgouros, G.; Bodei, L.; McDevitt, M.R.; Nedrow, J.R. Radiopharmaceutical Therapy in Cancer: Clinical Advances and Challenges. *Nat. Rev. Drug Discov.* **2020**, *19*, 589–608. [CrossRef] [PubMed]
2. Kesner, A.L.; Carter, L.M.; Ramos, J.C.O.; Lafontaine, D.; Olguin, E.A.; Brown, J.L.; President, B.; Jokisch, D.W.; Fisher, D.R.; Bolch, W.E. MIRD Pamphlet No. 28, Part 1: MIRDcalc-A Software Tool for Medical Internal Radiation Dosimetry. *J. Nucl. Med.* **2023**, *64*, 1117–1124. [CrossRef] [PubMed]
3. Peters, S.; Tran-Gia, J.; Agius, S.; Ivashchenko, O.V.; Badel, J.N.; Cremonesi, M.; Kurth, J.; Gabiña, P.M.; Richetta, E.; Gleisner, K.S.; et al. Implementation of Dosimetry for Molecular Radiotherapy; Results from a European Survey. *Phys. Medica* **2024**, *117*, 103196. [CrossRef] [PubMed]
4. Sjögreen-Gleisner, K.; Flux, G.; Bacher, K.; Chiesa, C.; de Nijs, R.; Kagadis, G.C.; Lima, T.; Georgosopoulou, M.L.; Gabiña, P.M.; Nekolla, S.; et al. EFOMP Policy Statement NO. 19: Dosimetry in Nuclear Medicine Therapy—Molecular Radiotherapy. *Phys. Medica* **2023**, *116*, 103166. [CrossRef] [PubMed]
5. Chiesa, C.; Strigari, L.; Pacilio, M.; Richetta, E.; Cannatà, V.; Stasi, M.; Marzola, M.C.; Schillaci, O.; Bagni, O.; Maccauro, M. Dosimetric Optimization of Nuclear Medicine Therapy Based on the Council Directive 2013/59/EURATOM and the Italian Law N. 101/2020. Position Paper and Recommendations by the Italian National Associations of Medical Physics (AIFM) and Nuclear Medicine (AIMN). *Phys. Medica* **2021**, *89*, 317–326. [CrossRef]
6. Finocchiaro, D.; Gear, J.I.; Fioroni, F.; Flux, G.D.; Murray, I.; Castellani, G.; Versari, A.; Iori, M.; Grassi, E. Uncertainty Analysis of Tumour Absorbed Dose Calculations in Molecular Radiotherapy. *EJNMMI Phys.* **2020**, *7*, 63. [CrossRef] [PubMed]
7. Gear, J.I.; Cox, M.G.; Gustafsson, J.; Gleisner, K.S.; Murray, I.; Glatting, G.; Konijnenberg, M.; Flux, G.D. EANM Practical Guidance on Uncertainty Analysis for Molecular Radiotherapy Absorbed Dose Calculations. *Eur. J. Nucl. Med. Mol. Imaging* **2018**, *45*, 2456–2474. [CrossRef] [PubMed]
8. Marcatili, S.; Pettinato, C.; Daniels, S.; Lewis, G.; Edwards, P.; Fanti, S.; Spezi, E. Development and Validation of RAYDOSE: A Geant4-Based Application for Molecular Radiotherapy. *Phys. Med. Biol.* **2013**, *58*, 2491–2508. [CrossRef] [PubMed]
9. Villoing, D.; Marcatili, S.; Garcia, M.-P.; Bardiès, M. Internal Dosimetry with the Monte Carlo Code GATE: Validation Using the ICRP/ICRU Female Reference Computational Model. *Phys. Med. Biol.* **2017**, *62*, 1885–1904. [CrossRef]
10. Stabin, M.G.; Sparks, R.B.; Crowe, E. OLINDA/EXM: The Second-Generation Personal Computer Software for Internal Dose Assessment in Nuclear Medicine. *J. Nucl. Med.* **2005**, *46*, 1023–1027. [CrossRef]
11. Andersson, M.; Johansson, L.; Eckerman, K.; Mattsson, S. IDAC-Dose 2.1, an Internal Dosimetry Program for Diagnostic Nuclear Medicine Based on the ICRP Adult Reference Voxel Phantoms. *EJNMMI Res.* **2017**, *7*, 88. [CrossRef] [PubMed]

12. Kayal, G.; Barbosa, N.; Marín, C.C.; Ferrer, L.; Fragoso-Negrín, J.-A.; Grosev, D.; Gupta, S.K.; Hidayati, N.R.; Moalosi, T.C.G.; Poli, G.L.; et al. Quality Assurance Considerations in Radiopharmaceutical Therapy Dosimetry Using PLANETDose: An International Atomic Energy Agency Study. *J. Nucl. Med.* **2024**, *65*, 125–131. [CrossRef] [PubMed]
13. Bensiali, M.; Anizan, N.; Leboulleux, S.; Lamart, S.; Davesne, E.; Broggio, D.; Desbrée, A.; Franck, D. Patient-Specific Biokinetics and Hybrid 2D/3D Approach Integration in OEDIPE Software: Application to Radioiodine Therapy. *Phys. Medica* **2023**, *113*, 102462. [CrossRef] [PubMed]
14. Fraass, B.; Doppke, K.; Hunt, M.; Kutcher, G.; Starkschall, G.; Stern, R.; van Dyke, J. American Association of Physicists in Medicine Radiation Therapy Committee Task Group 53: Quality Assurance for Clinical Radiotherapy Treatment Planning. *Med. Phys.* **1998**, *25*, 1773–1829. [CrossRef] [PubMed]
15. Mileva, M.; Marin, G.; Levillain, H.; Artigas, C.; van Bogaert, C.; Marin, C.; Danieli, R.; Deleporte, A.; Picchia, S.; Stathopoulos, K.; et al. Prediction of ^{177} Lu-DOTATATE PRRT Outcome Using Multimodality Imaging in Patients with Gastroenteropancreatic Neuroendocrine Tumors: Results from a Prospective Phase II LUMEN Study. *J. Nucl. Med.* **2024**, *65*, 236–244. [CrossRef]
16. Stabin, M.G.; Siegel, J.A. RADAR Dose Estimate Report: A Compendium of Radiopharmaceutical Dose Estimates Based on OLINDA/EXM Version 2.0. *J. Nucl. Med.* **2018**, *59*, 154–160. [CrossRef] [PubMed]
17. Sarrut, D.; Halty, A.; Badel, J.; Ferrer, L.; Bardiès, M. Voxel-based Multimodel Fitting Method for Modeling Time Activity Curves in SPECT Images. *Med. Phys.* **2017**, *44*, 6280–6288. [CrossRef] [PubMed]
18. Kayal, G.; Van, B.; Andl, G.; Tu, C.; Wareing, T.; Wilderman, S.; Mikell, J.; Dewaraja, Y.K. Linear Boltzmann Equation Solver for Voxel-level Dosimetry in Radiopharmaceutical Therapy: Comparison with Monte Carlo and Kernel Convolution. *Med. Phys.* **2024**. *Early View*. [CrossRef] [PubMed]
19. Grassi, E.; Fioroni, F.; Ferri, V.; Mezzenga, E.; Sarti, M.A.; Paulus, T.; Lanconelli, N.; Filice, A.; Versari, A.; Iori, M. Quantitative Comparison between the Commercial Software STRATOS® by Philips and a Homemade Software for Voxel-Dosimetry in Radiopeptide Therapy. *Phys. Medica* **2015**, *31*, 72–79. [CrossRef]
20. Grassi, E.; Fioroni, F.; Mezzenga, M.; Finocchiaro, D.; Sarti, M.A.; Filice, A.; Versari, A.; Iori, M. Impact of a Commercial 3D OSEM Reconstruction Algorithm on the 177Lu Activity Quantification of SPECT/CT Imaging in a Molecular Radiotherapy Trial. *Radiol Diagn Imaging* **2017**, *1*, 1–7. [CrossRef]
21. Sgouros, G.; Barest, G.; Thekkumthala, J.; Chui, C.; Mohan, R.; Bigler, R.E.; Zanzonico, P.B. Treatment Planning for Internal Radionuclide Therapy: Three-Dimensional Dosimetry for Nonuniformly Distributed Radionuclides. *J. Nucl. Med.* **1990**, *31*, 1884–1891. [PubMed]
22. Grassi, E.; Fioroni, F.; Berenato, S.; Patterson, N.; Ferri, V.; Braglia, L.; Filice, A.; Versari, A.; Iori, M.; Spezi, E. Effect of Image Registration on 3D Absorbed Dose Calculations in 177Lu-DOTATOC Peptide Receptor Radionuclide Therapy. *Phys. Med.* **2018**, *45*, 177–185. [CrossRef] [PubMed]
23. Ivashchenko, O.V.; O'Doherty, J.; Hardiansyah, D.; Cremonesi, M.; Tran-Gia, J.; Hippeläinen, E.; Stokke, C.; Grassi, E.; Sandström, M.; Glatting, G. Time-Activity Data Fitting in Molecular Radiotherapy: Methodology and Pitfalls. *Phys. Medica* **2024**, *117*, 103192. [CrossRef] [PubMed]
24. Fogliata, A.; Nicolini, G.; Clivio, A.; Vanetti, E.; Cozzi, L. Dosimetric Evaluation of Acuros XB Advanced Dose Calculation Algorithm in Heterogeneous Media. *Radiat. Oncol.* **2011**, *6*, 82. [CrossRef]